

ISSN 1996-5044

Research Journal of  
**Nanoscience**  
and Nanotechnology



## Research Article

# Humidity Sensor Based Nanocomposite Material

Karunesh Tiwari

Department of Physics, Babu Banarasi Das University, Lucknow, Uttar Pradesh, 226007 Pin, India

### Abstract

**Objective:** The objective was to synthesize nanocrystalline zinc titanate ( $\text{ZnTiO}_3$ ) via a solid-state reaction method and studied for its sensing behavior to humidity. Variations of resistance with relative humidity have been observed. **Methodology:** The surface morphology and structure of the synthesized material were characterized by SEM and XRD analysis, respectively. The structural analysis confirmed the formation of  $\text{ZnTiO}_3$  having an average crystallite size  $\sim 71$  nm with hexagonal structure at room temperature ( $21^\circ\text{C}$ ). Sensitivity of the sensing material as a function of time and concentration of the humidity was estimated. The sensitivity of the sensor at different temperatures has also been calculated. **Results:** The highest sensitivity observed at room temperature was  $17.86 \text{ M}\Omega/\% \text{RH}$ . The response and recovery times of sensing pellet were found  $\sim 180$  and  $\sim 500$  sec, respectively. The activation energy was calculated as  $0.024 \text{ eV}$ . **Conclusion:** These experimental results show that  $\text{ZnTiO}_3$  is a promising material for humidity sensor as comparable to previous reported materials.

**Key words:** Zinc oxide, titanium oxide, electrical properties, sensitivity, annealing

**Citation:** Karunesh Tiwari, 2017. Humidity sensor based nanocomposite material. Res. J. Nanosci. Nanotechnol., 7: 10-16.

**Corresponding Author:** Karunesh Tiwari, Department of Physics, Babu Banarasi Das University, Lucknow, Uttar Pradesh, 226007 Pin, India  
Tel: +91 9451037737

**Copyright:** © 2017 Karunesh Tiwari. This is an open access article distributed under the terms of the creative commons attribution License, which permits unrestricted use, distribution and reproduction in any medium, provided the original author and source are credited.

**Competing Interest:** The author has declared that no competing interest exists.

**Data Availability:** All relevant data are within the paper and its supporting information files.

## INTRODUCTION

ZnO based materials have been developed for various technological applications, such as humidity sensor, gas sensor and optoelectronic devices. Zinc Oxide shows different morphologies under difference processes of synthesis conditions whereby different properties are obtained for this metal oxide. ZnO powders reveal a needle like fine crystal 0.5 mm in width and 0.5-2 mm in length. TiO<sub>2</sub> is one of the most extensively studied metal oxides because of its remarkable optical and electrical properties. Zinc titanate is a promising candidate as dielectric materials<sup>1-3</sup>. It was reported that 3 compounds exist in ZnO-TiO<sub>2</sub> system, viz: Zn<sub>2</sub>TiO<sub>4</sub> (cubic) ZnTiO<sub>3</sub> (hexagonal) and Zn<sub>2</sub>Ti<sub>3</sub>O<sub>8</sub> (cubic)<sup>4-6</sup>. Among these compounds ilmenite-type hexagonal ZnTiO<sub>3</sub> compound has been reported to have superior electrical properties, dielectric constant of 19, Q = 3000 (at 10 GHz) and T<sub>r</sub> = 55 ppm/°C, which was very similar to that of the other ilmenite-types titanates<sup>7,8</sup>. Yadav *et al.*<sup>9</sup> obtained ZnTiO<sub>3</sub> (cubic) phase as precipitates inside the Zn<sub>2</sub>TiO<sub>4</sub> matrix having the same structure and lattice parameter as Zn<sub>2</sub>TiO<sub>4</sub> phase. Zinc orthotitanate Zn<sub>2</sub>TiO<sub>4</sub> can be prepared easily via the conventional solid state reaction of ZnO-TiO<sub>2</sub>. Due to dependence of diffusion coefficients of oxides on structure, surface area etc. crystallography and physical properties of the obtained particles can be changed by changing their morphology and particle size.

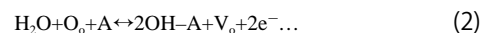
In the present study prepared compositions of 2 and 5 weight percentage of TiO<sub>2</sub> powder with ZnO and studied nanostructure and humidity sensing properties of these compositions. This was different compared to the work of Yildiz *et al.*<sup>10</sup> reported results of TiO<sub>2</sub>-ZnO compositions with lower weight% viz. 1, 2, 3 and 4% of TiO<sub>2</sub> powder in ZnO and discussed their microstructure properties and densification. Ismail *et al.*<sup>11</sup> have reported results with dopants of 1, 2 and 3% weight of (Al, Cu, I) powder with NO and discussed the micro structural, optical and electrical properties of NO by chemical spray pyrolysis. In earlier works, it was reported that morphological and humidity sensing studies of WO<sub>3</sub> mixed with ZnO and TiO<sub>2</sub> powders and optical humidity sensor based on titania films fabricated by sol gel and thermal evaporation<sup>12,13</sup>.

The average sensitivity of humidity sensor as the change in resistance ( $\Delta R$ ) of sensing element per unit change in relative humidity (RH%)<sup>14</sup>:

$$\text{Sensitivity} = \frac{(\Delta R)}{(\Delta \% RH)} \quad (1)$$

**Principle of operation of sensor:** NO and TiO<sub>2</sub> both are n-type semiconductors, hence sensitivity to humidity was a result of electronic conduction<sup>14,15</sup>. As semiconducting dry oxides of ZnO-TiO<sub>2</sub> nanocomposite are brought in contact with humid air, water molecules chemisorption on the available sites of the oxide surface. The adsorption of water molecules on the surface takes place via a dissociative chemisorption process which may be described in a two-step process as given below:

- Water molecules adsorbed on grain surface reacts with the lattice A (A → Zn or Ti) as:



Where, O<sub>o</sub> is the lattice oxygen and V<sub>o</sub> the vacancy created at the oxygen site according to the reaction:



- Doubly ionized oxygen, displaced from the lattice, reacts with the H<sup>+</sup> coming from the dissociation of water molecules to form a hydroxyl group as given below:



ZnO and TiO<sub>2</sub> both have electron vacancies. Because of this reaction, the electrons are accumulated at the ZnO/TiO<sub>2</sub> surface and consequently, the resistance of the sensing element decreases with increase in relative humidity.

The objective was to synthesize nanocrystalline zinc titanate via a solid-state reaction method and studied for its sensing behavior to humidity.

## MATERIALS AND METHODS

The study of humidity sensors based on ZnTiO<sub>3</sub> nanocomposite was carried out at Sensors and Materials Research Laboratory, University of Lucknow, Lucknow, in 2015.

**Sample preparation:** Two and 5% weight of TiO<sub>2</sub> powder (Qualigens, 99.9% pure) in ZnO (Qualigens, 99.9% pure) have been mixed uniformly for half an hour. 10% weight of glass powder has been added as binder to increase the strength of the sample. The powders have been pressed in pellet shape by uniaxially applying pressure of 260 MPa in hydraulic press machine at room temperature. The samples have been labeled S-0 (pure ZnO), S-2 (2 weight percentage of TiO<sub>2</sub> in ZnO) and S-5 (5 weight percentage of TiO<sub>2</sub> in ZnO), respectively. The

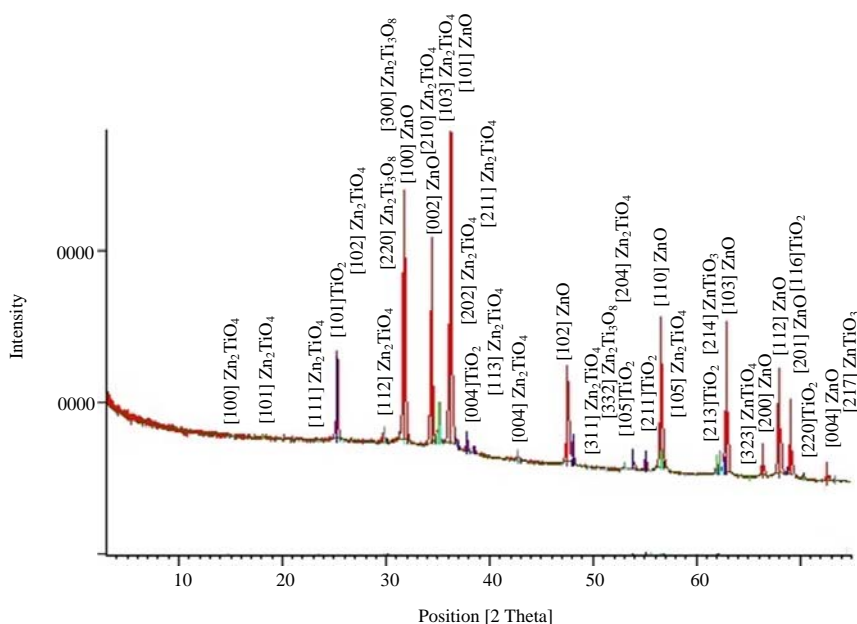


Fig. 1: XRD pattern of sample S-5 annealed at 500 °C

samples are having diameter of 8 mm and thickness 4 mm. The samples have been sintered in air at temperature of 200, 300, 400 and 500 °C for 3 h in an electric muffle furnace (Ambassador, India).

### Sample characterization

**X-ray diffraction analysis:** X-Ray diffraction has been studied using XPERT PRO-Analytical XRD system (Netherlands). The wavelength of the source used is 1.54060 Å. Figure 1 shows X-ray pattern for the sensing element S-5 annealed at 500 °C. The pattern shows extent of crystallization of the sensing element in the form of powder. The particle size for the sensing elements S-2 and S-5 calculated from Scherer's formula is 71 nm.

XRD pattern shows peaks of ZnO-TiO<sub>2</sub> binary system. In addition to these peaks, the pattern also manifests presence of large number of peaks of cubic Zn<sub>2</sub>TiO<sub>4</sub> (zinc orthotitanate) and some peaks of cubic Zn<sub>2</sub>Ti<sub>3</sub>O<sub>8</sub> and hexagonal ZnTiO<sub>3</sub> formed due to solid state reaction between TiO<sub>2</sub> and ZnO.

Some peaks of cubic Zn<sub>2</sub>Ti<sub>3</sub>O<sub>8</sub> and hexagonal ZnTiO<sub>3</sub> formed due to solid state reaction between TiO<sub>2</sub> and ZnO.

**Scanning electron microscopic (SEM) study:** The study of surface morphology of sensing elements has been carried out using Scanning Electron Microscope (LEO-430, Cambridge, England). Figure 2 shows SEM micrographs of nanocomposites of sensing element S-5, respectively,

annealed at temperature 500 °C. All the micrographs have been taken for the same magnification. The SEM micrographs show that the sensing elements manifest porous structure having grain size 207 nm with granulation and tendency to agglomerate.

Scanning micrographs show flakes of TiO<sub>2</sub> scattered throughout ZnO substrate forming a network of pores that are expected to provide sites for humidity adsorption. It can be observed that the particle density was getting increased with increase in the percentage weight of TiO<sub>2</sub> in ZnO. It seems as if the grain size of ZnO were getting inhibited with increasing composition of TiO<sub>2</sub>.

**Experimental characterization:** After sintering, the samples have been exposed to humidity in a humidity control chamber. Inside the humidity chamber, a thermometer ( $\pm 1^\circ\text{C}$ ) and standard hygrometer (Huger, Germany,  $\pm 1\%$  RH) are placed for the purpose of calibration. Variation in resistance has been recorded with change in relative humidity. Relative humidity has been measured using the standard hygrometer. Variation in resistance of the pellet has been recorded using a resistance meter (Sino meter,  $\pm 1\text{ M}\Omega$ , model: VC-9808). Copper electrode has been used to measure the resistance of the pellet. The resistance of the pellet has been measured normal to the cylindrical surface of the pellet. After studying humidity sensing properties, sensing elements have been kept in laboratory environment and their humidity sensing characteristics regularly monitored. To see the effect

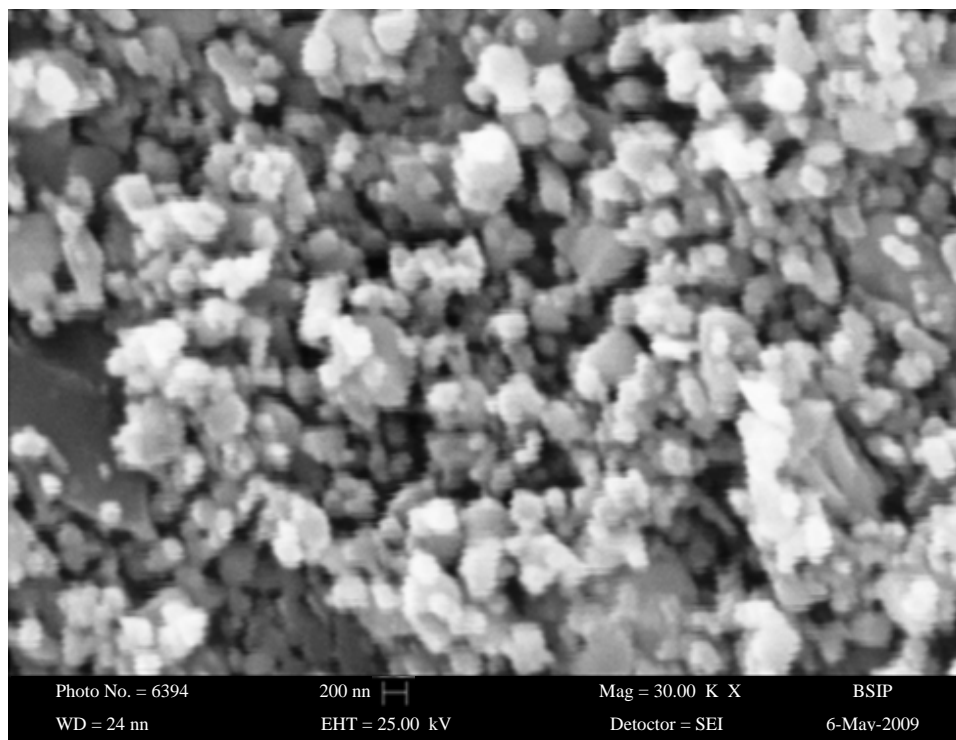


Fig. 2: SEM micrograph of sample S-5 annealed at 500°C

of ageing, the sensing properties of these elements have been examined again in the humidity control chamber after 6 months. The stability of the sensing element has been checked by keeping the sensing element at fixed values of RH% in the chamber and the values of resistance recorded as a function of time. The values have been found to be stable within  $\pm 3\%$  of the measured values.

**Temperature-resistance measurement:** In order to measure the variation of resistance with the temperature change a self made device has been used. In which temperature of the sample was increased and resistance of the sample was measured using 2 copper plates as electrodes and 2 thin copper wires as connecting leads at these temperatures. However, it should be mentioned that contact resistance could be assumed to be negligible owing to the high resistivity of the materials under consideration.

## RESULTS AND DISCUSSION

Variation of resistance of the sensing element has been recorded both for increasing and decreasing cycles of RH% for all sensing elements pure ZnO and 2 weight and 5 weight percentage of TiO<sub>2</sub> doped ZnO for annealing temperatures 200-500°C. It has been observed that all the sensing elements

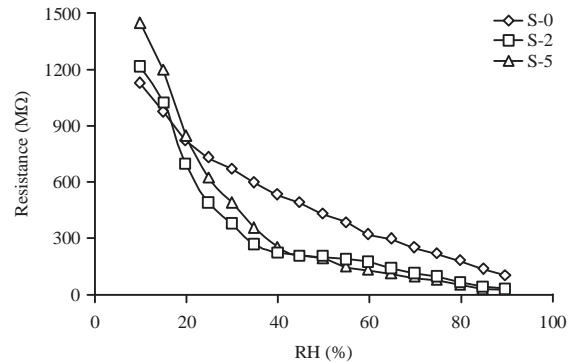


Fig. 3: Humidification graphs of the samples S-0, S-2 and S-5 annealed at 500°C

are showing lower hysteresis for annealing temperature 500°C. Hence, presented result for sensing elements pure ZnO and ZnO-TiO<sub>2</sub> for annealing temperature of 200-500°C. Figure 3 is the graph between the variations of the resistance of the sensing elements S-0, S-2 and S-5 with change in the value of the relative humidity after the sample has been annealed at 500°C. Figure 4 shows graph for variation of resistance with RH% of the sensing element S-5 for annealing temperature of 500°C. Figure 4 is the graph for increasing cycle of percentage RH and graph for decreasing cycle of percentage RH. In increasing cycle, the resistance was

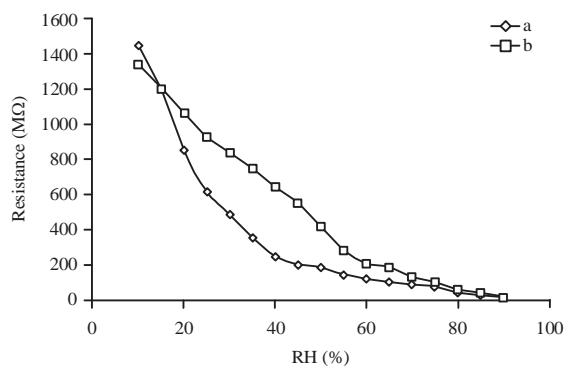


Fig. 4: Hysteresis graph for sample S-5 annealed at 500°C

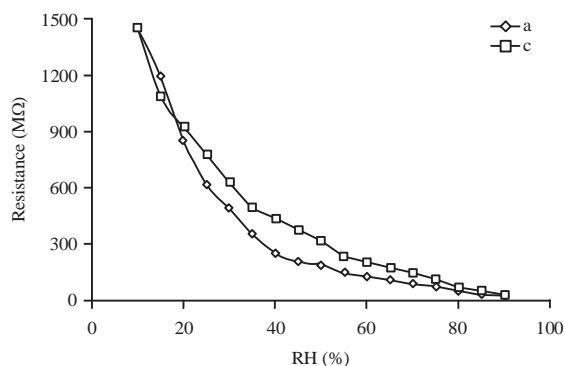


Fig. 5: Repeatability graph for sample S-5 after 6 months annealed at 500°C

found to decrease by 87% for increase in relative humidity from 10-50% RH. In decreasing cycle, the resistance decreases by 68.6% in this range of 10-50% RH. In the range of 50-90% RH resistance decreases by 89.3 and 95.2%, respectively for increasing and decreasing cycle of relative humidity. The average sensitivity was the range of 10-50%, RH is 31.47 and 4.20 M/%RH in the range of 50-90% RH. Pandey *et al.*<sup>16</sup> find out that element with 15 weight percentage of TiO<sub>2</sub> in ZnO shows best results with a sensitivity of 9.08 MΩ/%RH in 10-90% relative humidity range.

Figure 5 is the graph for the increasing cycle of relative humidity and the graph for the increasing cycle of the relative humidity corresponding to the same experiment repeated after 6 months. From the graph of

Fig. 5, the resistance was found to decrease by 87% for increase in the relative humidity from 10-50% RH whereas resistance decreases by 89.3% in the range 50-90%.

The average sensitivity was the range of 10-50%, RH is 31.47 and 4.20 M/%RH in the range of 50-90% RH. The phenomenon of hysteresis may be attributed to the initial chemisorption on the surface of the sensing element. This chemisorbed layer, once formed was not further affected by exposure to or removal of humidity, it can be thermally desorbed only. Hence, in the decreasing cycle of percentage RH, the initially adsorbed water was not removed fully leading to hysteresis. It is observed from Table 1 that the sensing element S-5 shows the value of highest sensitivity of 17.83 MΩ/%RH in the increasing cycle of percentage RH and 16.55 MΩ/%RH in the decreasing cycle of percentage RH. Thus the hysteresis in the value of sensitivity for sensing elements S-5 was 7.17% whereas, for S-0 and S-2 these values are 33 and 16%, respectively. Pandey *et al.*<sup>17</sup> worked 20% of Cu<sub>2</sub>O doped in ZnO showed best results with sensitivity up to 4.78 MΩ/%RH for annealing temperature of 400°C.

When these observations have been repeated after 6 months, it was found that variations in both ranges (i.e., 10-50% and 50-90% RH) are nearly same. From the graph of Fig. 5, the resistance was found to decrease by 78.2% for increase in the relative humidity from 10-50% RH, whereas, resistance decreases by 89.2% in the range 50-90%. The average sensitivity was the range of 10-50%, RH is 28.45 and 7.07 M/%RH in the range of 50-90% RH. After 6 months it was seen that from 10-90% RH resistance was decreased by 97.6% and average sensitivity becomes 17.76 M/%RH. It may be concluded that both the graphs are showing almost similar behavior in the range 10-90% of relative humidity. Srivastava and Yadav<sup>18</sup> reported that curve for ZnO-Nb<sub>2</sub>O<sub>5</sub> sensing element shows that as RH increases, resistance decreases markedly up to 65% RH which gives maximum slope having maximum average sensitivity 23 MΩ/%RH.

Figure 6 shows the graph sensitivity vs temperature for sensing element S-5 for annealing temperature 200-500°C. The graph shows the maximum value of sensitivity for sensing element TiO<sub>2</sub> doped ZnO.

Table 1: Sensitivity (MΩ/%RH) of sensing elements for different annealing temperatures

Temperature (°C)	RH%	S-5		
		a	b	c
200	10-90	16.43	17.15	16.50
300	10-90	16.86	17.07	16.70
400	10-90	17.30	17.10	17.03
500	10-90	17.86	16.55	17.76

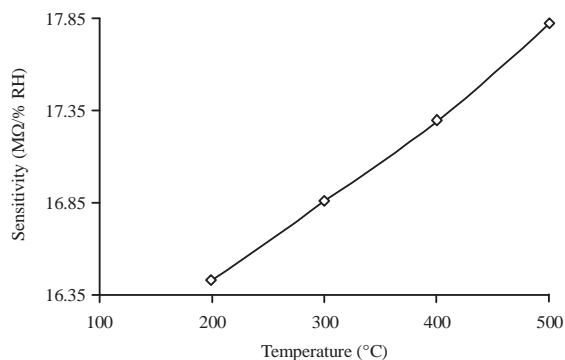


Fig. 6: Sensitivity vs. temperature for sample S-5

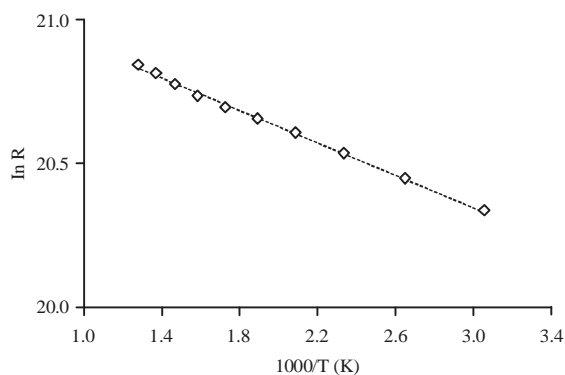


Fig. 7: Arrhenius plot of sample S-5

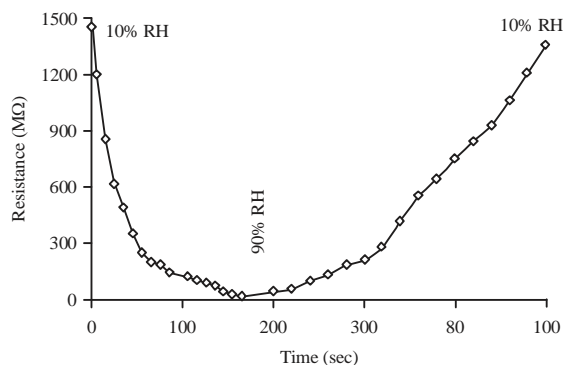


Fig. 8: Response and recovery time of sample S-5

**Activation energy:** Activation energy has been measured from the Arrhenius plot for resistance. Arrhenius plot was measured between the  $\log_e R$  and  $1000/T$ . The temperature dependence of the resistance is shown from the relation  $R = R_0 \exp(E_a/kT)$  where,  $E_a$  is the activation energy<sup>15</sup>. Figure 7 shows the Arrhenius plot for resistance. Activation energy measured from Arrhenius plot in 50-500°C range is found to be 0.024 eV.

**Response and recovery time:** The time taken to accomplish 90% of the total resistance variation is defined as

response/recovery time during the RH increasing and decreasing processes. Figure 8 shows the variation of resistance with time. The response time and recovery time of the best sample S-5 are 180 and 500 sec, respectively.

Values of sensitivity calculated for sensing elements pure ZnO and ZnO-TiO<sub>2</sub> for annealing temperatures 200, 300, 400 and 500°C are shown in Table 1. Column a represents value of sensitivity for increasing cycle, column b represents value of sensitivity for decreasing cycle of percentage RH and column c represents value of sensitivity for increasing cycle after 6 months. Pandey *et al.*<sup>19</sup> reported study of pure ZnO sensing element showed the values of activation energy from the Arrhenius plot is 0.041 eV for temperature range 200- 400°C and 0.393 eV for temperature range 400-500°C. The sensing element of ZnO shows best results with sensitivity of 11.13 MΩ/%RH for the annealing temperature of 400°C<sup>19</sup>. These finding are with agreement of present study in which 10-90% RH resistance was decreased by 97.6% and average sensitivity becomes 17.76 M/%RH for annealing temperature of 400°C at room temperature that shows better sensitivity than the earlier.

It was understood that the increase in the conductivity of the sample with relative humidity in the lower range (<40% RH) was due to the adsorption of the water molecules on the pellet surface with capillary nanopores. Higher porosity increases surface to volume ratio of the materials and enhances diffusion rate of water into or out-off the porous structure and thus, helps in getting good sensitivity. At high relative humidity (>40% RH), liquid water condenses in the capillary like pores, forming a liquid like layer. A further rise in electrical conductivity occurs due to electrolytic conduction in addition to the protonic transport in the adsorbed layer.

## CONCLUSION

It is concluded that as annealing temperature is increased sensitivity of the samples increases. The maximum hysteresis for best sample i.e., S-5 is less than 8% RH. Change in resistance with humidity is seen up to about 3 orders. The average sensitivity of this sample is 17.86 MΩ/%RH. Activation energy is found to be 0.024 eV. Response and recovery time for the best sample is found to be 180 and 500 sec, respectively. This study confirms that sample annealed at 500°C is the best sample among all samples. This sensing element shows good reproducibility, low hysteresis and less effect of aging. The XRD pattern of this sensing element shows large number of peaks of cubic Zn<sub>2</sub>TiO<sub>4</sub> and some peaks of cubic Zn<sub>2</sub>Ti<sub>3</sub>O<sub>8</sub> and ZnTiO<sub>3</sub> formed due to solid state reaction between TiO<sub>2</sub> and ZnO. The SEM micrographs show that the sensing elements manifest porous structure.

## SIGNIFICANCE STATEMENTS

This study discovers the resistive type humidity sensor based on ZnTiO<sub>3</sub> nanocomposite material that can be beneficial for industry and helpful for environmental monitoring to measure humidity. Present study is differ from other due to use of high weight percentage of TiO<sub>2</sub> in ZnO for the purpose of humidity sensing over the entire range of humidity (10-90% RH) and it showed better activation energy in the temperature range 50-500°C due to their nanostructured surface morphology and lower particle size ~71 nm. This study will help the researcher to uncover the critical areas of resistive type humidity sensors based on nanocomposites materials that many researchers were not able to explore. Thus a new theory on ZnTiO<sub>3</sub> nanocomposite, humidity sensor and nanomaterials may be arrived at.

## ACKNOWLEDGMENT

Author would like to thank the Geological Survey of India, Lucknow for providing XRD facility and B.S.I.P. Lucknow for providing SEM facility.

## REFERENCES

1. Shimizu, Y., H. Arai and T. Seiyama, 1985. Theoretical studies on the impedance-humidity characteristics of ceramic humidity sensors. *Sens. Actuators*, 7: 11-22.
2. Fagan, J.G. and V.R.W. Amarakoon, 1993. Reliability and reproducibility of ceramic sensors. I-NTC thermistors. *Am. Ceram. Soc. Bull.*, 72: 70-79.
3. Yarkin, D.G., 2003. Impedance of humidity sensitive metal/porous silicon/n-Si structures. *Sens. Actuators A: Phys.*, 107: 1-6.
4. Tailoka, F., D.J. Fray and R.V. Kumar, 2000. Humidity sensing under aggressive conditions using nafion conductors. *Ionics*, 6: 383-388.
5. Gu, L., Q.A. Huang and M. Qin, 2004. A novel capacitive-type humidity sensor using CMOS fabrication technology. *Sens. Actuators B: Chem.*, 99: 491-498.
6. Cantalini, C. and M. Pelino, 1992. Microstructure and humidity-sensitive characteristics of  $\alpha$ -Fe<sub>2</sub>O<sub>3</sub> ceramic sensor. *J. Am. Ceram. Soc.*, 75: 546-551.
7. Wang, W. and A.V. Virkar, 2004. A conductimetric humidity sensor based on proton conducting perovskite oxides. *Sens. Actuators B: Chem.*, 98: 282-290.
8. Lee, S.P. and K.J. Park, 1996. Humidity sensitive field effect transistors. *Sens. Actuators B: Chem.*, 35: 80-84.
9. Yadav, B.C., R. Srivastava and C.D. Dwivedi, 2008. Synthesis and characterization of ZnO-TiO<sub>2</sub> nanocomposite and its application as a humidity sensor. *Philos. Mag.*, 88: 1113-1124.
10. Yildiz, K., N. Karakus, N. Toplan and H.O. Toplan, 2007. Densification and grain growth of TiO<sub>2</sub>-doped ZnO. *Mater. Sci. Poland*, 25: 1135-1142.
11. Ismail, R.A., A. Al-Naimi and A.A. Al-Ani, 2006. Preparation and characteristics study of ZnO: (Al, Cu, I) thin films by chemical spray pyrolysis. *e-J. Surface Sci. Nanotechnol.*, 4: 636-639.
12. Pandey, N.K., A. Tripathi, K. Tiwari, A. Roy and A. Rai *et al.*, 2008. Morphological and humidity sensing studies of WO<sub>3</sub> mixed with ZnO and TiO<sub>2</sub> powders. *Sens. Transducers J.*, 96: 42-46.
13. Yadav, B.C., N.K. Pandey, A. Srivastava and P. Sharma, 2007. Optical humidity sensors based on titania films fabricated by sol-gel and thermal evaporation methods. *Measur. Sci. Technol.*, 18: 260-264.
14. Pandey, N.K., K. Tiwari and A. Roy, 2011. Ag doped WO<sub>3</sub> nanomaterials as relative humidity sensor sign in or purchase. *IEEE Sens. J.*, 11: 2911-2918.
15. Kuang, Q., C. Lao, Z.L. Wang, Z. Xie and L. Zheng, 2007. High-sensitivity humidity sensor based on a single SnO<sub>2</sub> nanowire. *J. Am. Chem. Soc.*, 129: 6070-6071.
16. Pandey, N.K., K. Tiwari and A. Roy, 2012. ZnO-TiO<sub>2</sub> nanocomposite: Characterization and moisture sensing studies. *Bull. Mater. Sci.*, 35: 347-352.
17. Pandey, N.K., K. Tiwari and A. Roy, 2011. Moisture sensing application of Cu<sub>2</sub>O doped ZnO nanocomposites. *IEEE Sens. J.*, 11: 2142-2148.
18. Srivastava, R. and B.C. Yadav, 2012. Nanostructured ZnO, ZnO-TiO<sub>2</sub> and ZnO-Nb<sub>2</sub>O<sub>5</sub> as solid state humidity sensor. *Adv. Mater. Lett.*, 3: 197-203.
19. Pandey, N.K. and K. Tiwari, 2010. Morphological and relative humidity sensing properties of pure ZnO nanomaterial. *Sens. Transducers J.*, 122: 9-19.